ACS APPLIED MATERIALS & INTERFACES

Research Article

www.acsami.org

Adsorption and Hydrolytic Activity of the Polycatalytic Cellulase Nanocomplex on Cellulose

Ranjan K. Kamat,[†] Wanfu Ma,[‡] Yongkun Yang,[†] Yuting Zhang,[‡] Changchun Wang,[‡] Challa V. Kumar,[§,∥] and Yao Lin*[,†,§]

[†]Polymer Program, Institute of Material Science, [§]Department of Chemistry, and [∥]Department of Molecular and Cellular Biology, University of Connecticut, Storrs, Connecticut 06269, United States

[‡]State Key Laboratory of Molecular Engineering of Polymers and Department of Macromolecular Science, Fudan University, Shanghai 200433, China

Supporting Information

ABSTRACT: The formation of polycatalytic enzyme complexes may enhance the effectiveness of enzymes due to improved substrate interaction and synergistic actions of multiple enzymes in proximity. Much effort has been made to develop highly efficient polycatalytic cellulase complexes by immobilizing cellulases on low-cost polymer or nanoparticle scaffolds, aiming at their potential applications in biomass conversion to fuels. However, some key cellulases carry out the hydrolytic reaction on crystalline cellulose in a directional, processive manner. A large, artificial polycatalytic complex is unlikely to undergo a highly coordinated motion to slide on the cellulose surface as a whole unit. The mechanism underlying the activity enhancements observed in some artificial cellulase complexes and the limit of this approach remain elusive. Herein, we report the synthesis of polycatalytic cellulase complexes bound to colloidal polymer nanoparticles with a magnetic core and describe their unique adsorption, hydrolytic activities, and motions on cellulose. The polycatalytic clusters of cellulases on colloidal polymers show an increased rate of hydrolytic reactions on cellulose, but this was observed mainly at relatively low cellulase-to-cellulose ratios. Enhanced efficiency is mainly attributed to increased local concentrations of cellulases on the scaffolds and their polyvalent interactions with cellulose. However, once bound, the polycatalytic complexes can only carry out reactions locally and are not capable of relocating to new sites rapidly due to their lack of long-range surface mobility and their extremely tight binding. The development of highly optimized polycatalytic complexes may arise by developing novel nanoscaffolds that induce concerted motion of the complex as a whole.

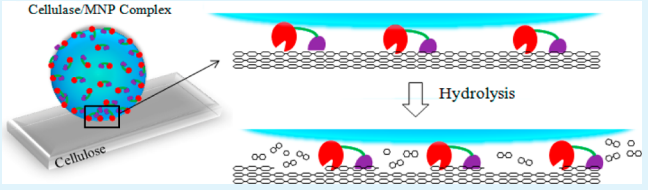

KEYWORDS: *cellulase, enzyme complexes, magnetic nanoparticles, multivalent interactions, enzymatic activity, biomass conversion*

INTRODUCTION

One key challenge in converting biomass to fuels is the recalcitrant nature of cellulosic materials against chemical and enzymatic degradation.[1−5] Natural celluloses (e.g., in plant cell walls) are made of water-insoluble, semi-crystalline polysaccharide polymers stabilized by extensive intra- and interchain hydrogen bonds, which provide resistance to hydrolysis. To enhance the efficiency of enzymatic hydrolysis of cellulose, much effort has been made on improving the biological activities of individual cellulases by protein engineering and the design of cellulase cocktails consisting of multiple cellulases and helper enzymes for synergistic actions on recalcitrant cellulose.[6−8] On the other hand, the multicatalytic enzyme complexes found in some anaerobic bacteria, called cellulosomes, conduct efficient hydrolysis of recalcitrant cellulose.[9−12] Cellulosomes consist of a protein scaffold "scaffoldin" to organize 6−14 enzyme units into a large catalytic assembly, wherein different catalytic units work in a concerted manner.[9−12] Activities of natural cellulosomes are an order of magnitude higher than a corresponding mixture of individual cellulolytic enzymes in the absence of scaffoldin. Increased activity of cellulosome has been generally attributed to the proximity of different synergistic enzymes and improved substrate binding in the integrated supramolecular structure of the cellulosome. Inspired by the remarkable efficiency of natural cellulosomes, artificial organization of 2−4 cellulolytic enzymes into cellulosome chimeras (e.g., "minicellulosomes") has shown to result in characteristically higher activities on recalcitrant substrates.[13,14] Further extension of the artificial cellulosome concept led to the recent efforts in integrating the industrial cellulases (e.g., produced from Fungi rather than bacteria) with a variety of nanoscaffolds to assemble multi- or polycatalytic cellulase complexes, which resulted in enhanced activities or stabilities.[15−22]

The cellulosome-inspired complexes were made by immobilization of industrial cellulases on low cost synthetic polymer or nanoparticle scaffolds, and they are technologically attractive due to the simple process involved in the material synthesis, the recyclability of the nanoscaffolds, and the scale-up potential for

Received: May 20, 2013
Accepted: August 6, 2013
Published: August 22, 2013

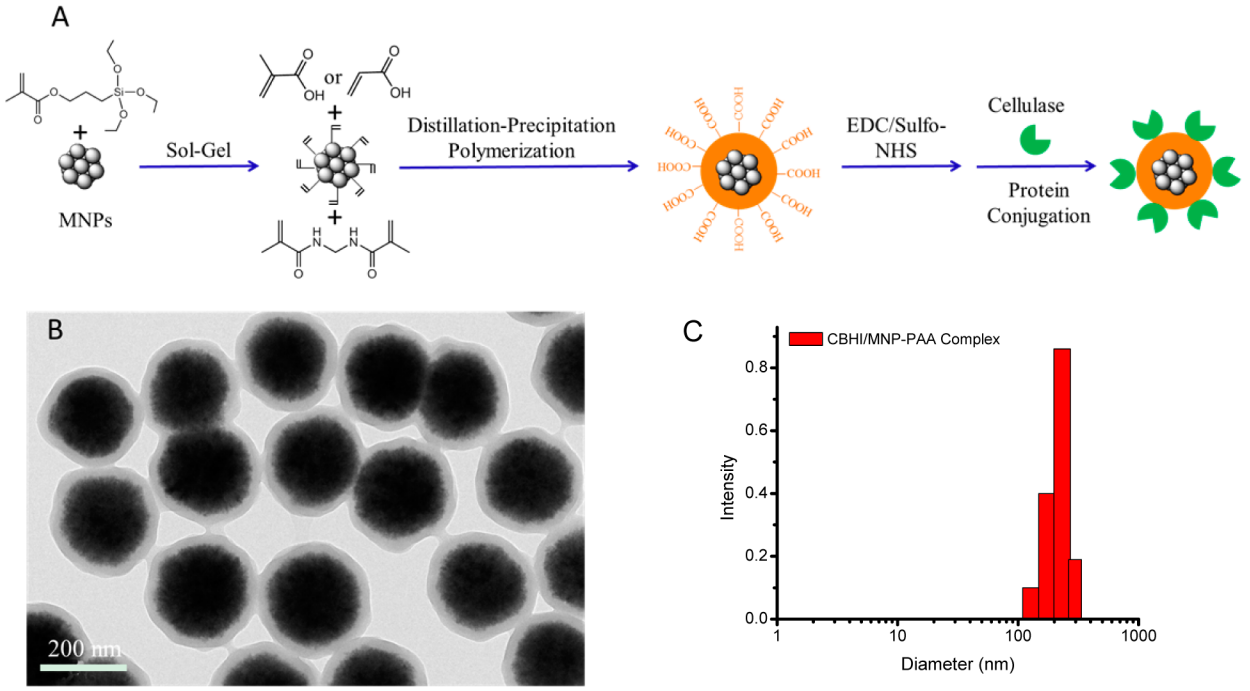

Figure 1. (A) Schematic of the synthesis of MNP−PAA or MNP−PMAA core−shell particles and the formation of polycatalytic complexes by conjugation of cellulases on the surface of the particle. (B) The representative TEM image of the CBHI/MNP−PAA complexes. (C) The distribution of their hydrodynamic radius measured by dynamic light scattering.

biorefinery applications. Unlike the cellulolytic enzymes in cellulosomes, the industrial cellulases such as *Trichoderma reesei* cellobiohydrolase I (CBHI) are produced by fungi. Many of these fungal cellulases have evolved into a two-domain structure, consisting of a catalytic domain (CD) and a cellulose binding domain (CBD) connected by a peptide linker.[23−28] The cellulases such as CBHI often carry out the hydrolytic reactions in a processive manner—i.e., the enzyme remains bound and "slides" along the polysaccharide chain that has been previously separated from the crystalline cellulose lattice.[29,30] A large, artificial polycatalytic complex consisting of tens to hundreds of immobilized enzyme units is unlikely to undergo a highly coordinated motion to slide on the cellulose surface as a whole unit. If polycatalytic complexes show activity enhancements, then what are the mechanisms underlying such behavior? This is a critical question that needs to be addressed before artificial cellulosomes can be rationally designed to achieve maximal hydrolytic efficiency.

To address this question in the current study, we synthesized polycatalytic cellulase complexes with artificial scaffold nanomaterials, examined their adsorption and hydrolytic activities on cellulose, and compared their performance to the corresponding cellulases in their free state. We identified specific ranges of reaction conditions (e.g., low feeding enzyme-to-substrate ratios), in which the artificial polycatalytic cellulase complexes have significant advantages over freely dispersed cellulases. The study shows that the enhanced hydrolytic efficiency is attributed to increased local concentrations of cellulases on the scaffolds and their polyvalent interactions with cellulose, particularly at low enzyme loadings on the substrate. The current results bring us one step closer to the rational design of artificial cellulosomes to overcome the current bottleneck in the use of recalcitrant biomass for the economic production of biofuels.

RESULTS AND DISCUSSION

Synthesis of Polycatalytic Cellulase Complexes on Colloidal Polymers with a Magnetic Core. Industrial cellulolytic enzymes produced from *Trichoderma reesei* (Novozyme Celluclast, purchased from Sigma-Aldrich) were purified to homogeneity by GE FPLC AKTA Purifier equipped with ion-exchange columns (see Supporting Information, Figure S1). The major cellulolytic enzymes (e.g., cellobiohydrolase I (CBHI)) were identified based on their molecular weights and their specific activities (Figure S1, Supporting Information). To unambiguously determine the effect of polycatalytic structures on the hydrolytic efficiency on cellulose, cellulase complexed with the polymer scaffolds is to be completely separated from free enzymes and quantified under the experimental conditions. To address this challenge, we developed a polycatalytic system consisting of cellulases covalently linked on the surface of colloidal polymers with a magnetic nanoparticle (MNP) core. The MNP−polymer core−shell structures were synthesized through encapsulating γ-methacryloxypropyltrimethoxysilane (MPS) modified Fe_3O_4 nanocrystal clusters with a crosslinked hydrophilic polymer shell (Figure 1A) using the method we previously reported.[31,32] MNP provides a convenient handle to separate the complex, while the colloidal polymer would serve as a benign scaffold to attach the enzymes. In the approach, MNPs with diameter of 200 ± 30 nm were first prepared by a solvothermal process at 200 °C and modified with MPS on the surface. A one-step distillation−precipitation polymerization (DPP) of acrylic acid (AA) or methylacrylic acid (MAA) with *N*,*N*′-methylenebisacrylamide (MBA) was used to prepare well-defined core−shell structure with high magnetization susceptibility and large surface density of carboxyl groups (Figure 1B). The polymer shell thickness and the degree of crosslinking were controlled by adjusting the feeding amount of AA or MAA monomers, MBA crosslinker, and 2,2′-azobisisobutyronitrile (AIBN) initiator. MNP−PAA and MNP−PMAA with a MNP

dx.doi.org/10.1021/am401916k | ACS Appl. Mater. Interfaces 2013, 5, 8486−8494

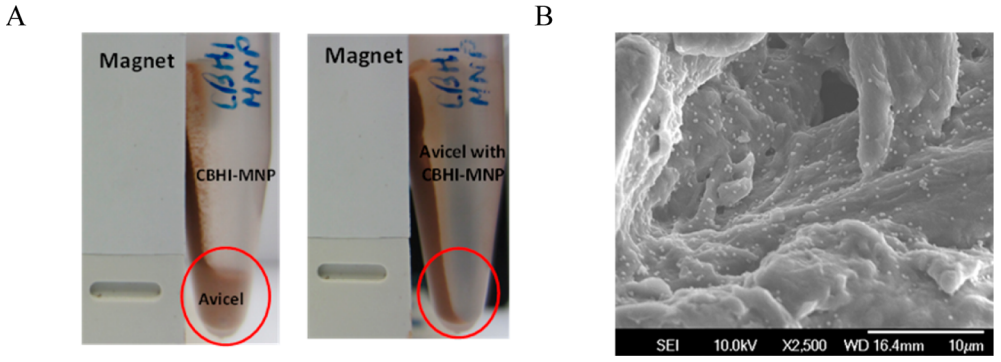

Figure 2. Adsorption of polycatalytic cellulase complexes on Avicel cellulose. (A) The response of Avicel cellulose to magnet before (left panel) and after (right panel) incubation with CBHI/MNP−PAA for 2 h. (B) FESEM image of CBHI/MNP−PAA (bright dots in the image) on Avicel. Samples were incubated with CBHI/MNP−PAA for 6 h and washed 5 times with Tris-HCl buffer.

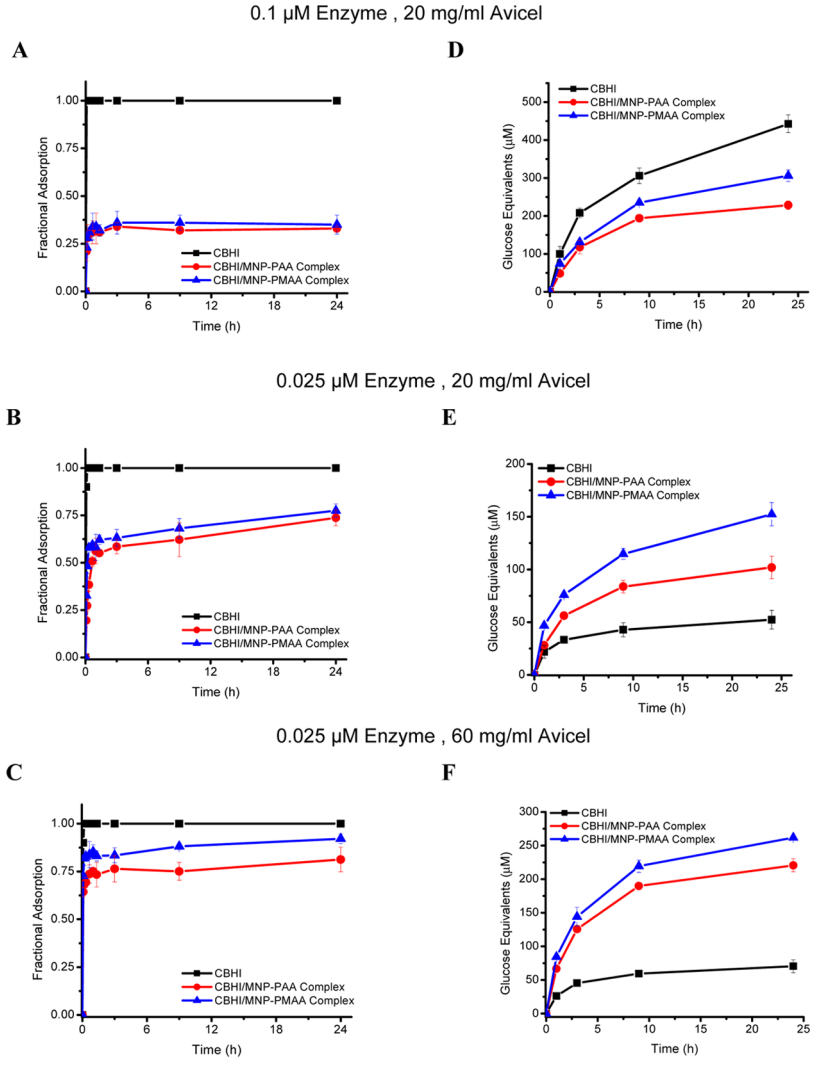

Figure 3. Adsorption kinetics (A−C) and hydrolysis kinetics (D−F) of Avicel by CBHI in the free state (as black square), CBHI/MNP−PAA complex (as red circle), and CBHI/MNP−PMAA complex (as blue triangle). Initial concentrations of total enzymes and Avicel are as indicated. Incubation was at 37 °C in 5 mM Tris-HCl, pH 6.5. At the given times, Avicel was separated from the enzyme complexes or the free enzyme by sedimentation. The supernatant was used to determine concentrations of unbound complexes/enzymes and soluble sugar.

core of 200 ± 30 nm in diameter and a polymer shell of 30 ± 10 nm in thickness and 10% crosslinking were prepared as the scaffold materials.

The carboxyl groups of the PAA and PMAA were then activated for conjugation of cellulase by standard carbodiimide coupling chemistry to produce cellulase/MNP−PMAA and cellulase/MNP−PAA complexes.[33] The complexes are separated from unbound enzymes within 30 s by a standard magnetic separation rack. The surface densities of CBHI on MNP−PMAA or MNP−PAA particles were measured by an enzymatic assay

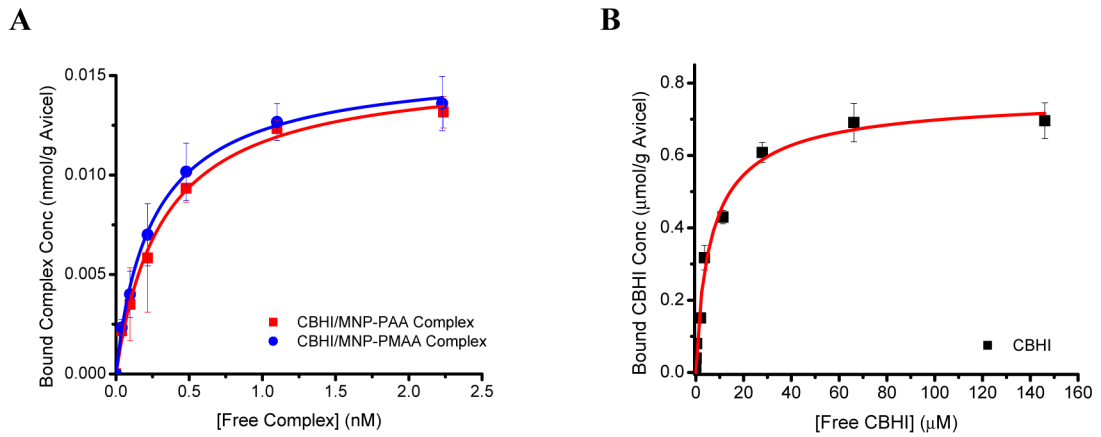

Figure 4. Adsorption of polycatalytic cellulase complexes on Avicel cellulose. Adsorption isotherms of the (A) CBHI/MNP−PAA complex, CBHI/MNP−PMAA complex, and (B) CBHI on Avicel. Avicel concentration was kept constant (20 mg/mL), at increasing enzyme concentrations.

Table 1. Mean binding affinity, binding capacities and the heterogeneity index for the adsorption of the polycatalytic complexes and the CBHI to Avicel

sample	[a]mean binding affinity (M^{-1})	[b]binding capacity (μmol enzyme/g Avicel)	heterogeneity index
CBHI/MNP−PAA	$(3.1 \pm 0.6) \times 10^9$	0.0046 ± 0.0004	0.99 ± 0.11
CBHI/MNP−PMAA	$(4.1 \pm 0.4) \times 10^9$	0.0045 ± 0.0001	1.02 ± 0.06
CBHI	$(1.4 \pm 0.3) \times 10^5$	0.77 ± 0.04	0.86 ± 0.09

[a]The binding affinity of CBHI/MNP−PAA or CBHI/MNP−PMAA is expressed on the basis of the concentration of particles. [b]To compare with CBHI, the binding capacity for the CBHI/MNP−PAA or CBHI/MNP−PMAA is expressed on the basis of the number of CBHI enzyme molecules.

using 4-methylumbelliferyl-β-D-cellobioside as the fluorescent soluble substrate[34] (Figure S2, Supporting Information). The reaction conditions were optimized to obtain the CBHI complex containing around ~300 enzymes per complex for the initial tests. TEM and dynamic light scattering (DLS) data were used to determine the size distributions of the particles after enzyme conjugation (Figure 1C), and there was no aggregation. These polycatalytic cellulase−particle complexes were then used as the model system to evaluate polycatalytic effects, as they are free of contributions from unbound enzymes.

Adsorption and Reactions of Polycatalytic CBHI Complexes on Cellulose. CBHI is the dominant cellulase of fungi and is capable of completely hydrolyzing the highly crystalline *Valonia* cellulose by itself.[6,35,36] Therefore, we focused on the polycatalytic CBHI complexes in this study. CBHI/MNP−PAA and CBHI/MNP−PMAA were made by conjugating CBHI on MNP−PAA and MNP−PMAA, respectively, and magnetically separated from unbound CBHI. The system is thus free of interference from individual freely dispersed enzymes, either before or after their adsorption on the cellulose. We chose Avicel which is a microcrystalline cellulose with 60−80% crystallinity as the targeted substrate.[37] Upon mixing CBHI−MNP complexes with Avicel, the complexes adsorbed on the surface of Avicel and facilitated the magnetic separation of Avicel particles (Figure 2A) as the complexes are strongly adhered to the Avicel surface. The distribution of the complexes on the surface of Avicel is shown in the field emission scanning electron microscopy (FESEM) (Figure 2B).

The kinetics of adsorption to Avicel and subsequent hydrolytic reactions to release soluble sugar (cellobiose and glucose) were followed at 37 °C using different initial concentrations of CBHI/MNP−PAA, CBHI/MNP−PMAA, and CBHI and enzyme-to-substrate ratios. The time courses of adsorption as a fraction of total enzyme and the amount of soluble sugars released are presented in Figure 3. The attachment of CBHI onto polycatalytic complexes changed both adsorption and activity, relative to those of CBHI.

Compared to the rate of adsorption of CBHI, the binding of CBHI/MNP−PAA and CBHI/MNP−PMAA to Avicel was slower and required more than 2 h to reach saturation. The process depended on the concentrations of enzyme and Avicel (Figure 3A−C). At the same Avicel concentration, the adsorption of CBHI complexes is lower than adsorption of CBHI. Increasing the Avicel concentration enhanced the adsorption level of the enzyme complexes (Figure 3C), with up to 85% adsorption reached at an Avicel concentration of 60 mg/mL (or ~6 wt %). In all cases, the overall adsorption was not affected as hydrolysis of Avicel proceeded.

Analysis of the Adsorption Isotherms. The adsorption isotherms with 20 mg/mL of Avicel at 37 °C are shown in Figure 4. The complex concentrations in Figure 4A were determined by dividing the molarity of complexed CBHI with the estimated number of CBHI per particle. Due to the heterogeneous nature of the Avicel surface and different binding characteristics of free and noncomplexed CBHI, the Langmuir−Freundlich (LF) model was used to analyze the adsorption isotherms.[38] The LF isotherm is able to model the adsorption behavior of both homogeneous and heterogeneous systems and is suitable for the comparisons of adsorption with very different underlying mechanisms. The binding parameters can be determined directly using the LF fitting coefficients that yield a measure of the total number of binding sites, mean binding affinity, and heterogeneity.[38] The equation for the LF model is as follows;

$$B = \frac{N_t a F^m}{1 + aF^m} \quad (1)$$

where B and F are equilibrium concentration of bound and unbound enzymes or enzyme complexes; N_t is the maximum binding capacity; and m is the heterogeneity index, which varies from 0 to 1 (e.g., $m = 1$ for a homogeneous material and $m < 1$ for

dx.doi.org/10.1021/am401916k | ACS Appl. Mater. Interfaces 2013, 5, 8486−8494

a heterogeneous material). The variable a is related to the mean binding affinity (K_A) as $K_A = a^{1/m}$. On the basis of the LF model, the mean binding affinity, the maximal binding capacities, and the heterogeneity index (equivalent to the inverse of the cooperativity factor in a Hill equation) were derived from the adsorption isotherms (Table 1).

Table 1 shows that the binding affinities of CBHI/MNP−PAA and CBHI/MNP−PMAA are several orders of magnitude higher than that of CBHI. Such tight binding indicates that the polycatalytic complex is bound to Avicel through multivalent interactions and almost irreversible in practice. The maximal binding capacity for CBHI/MNP−PAA and CBHI/MNP−PMAA is similar but about 160 times lower than that of CBHI. Normally, high surface binding capacity will require some rearrangement of the molecules that are already bound to the surface,[39] to optimize the distribution of molecules for higher coverage. The simultaneous low binding capacity and high apparent affinity found for the CBHI complexes suggest the lack of mobility of the complexes on Avicel or the existence of strong negative cooperativity in the binding process (e.g., through electrostatic repulsion from the net charges of large complexes). The heterogeneity index obtained from fitting the binding isotherms to the LF model is found to be less than 1 for the CBHI, as expected from the heterogeneous nature of the Avicel surface, which contains different types of binding sites.[6] In contrast, the heterogeneity indexes for both CBHI complexes were found to be around 1. Unlike CBHI, these large complexes cannot distinguish the heterogeneous nature of the Avicel surface, as the binding is the collective behavior of a large number of CBHI enzymes in the complex.

Hydrolytic Efficiency of Polycatalytic CBHI Complexes on Cellulose. Figure 3D−F compares the apparent hydrolytic efficiency of CBHI complexes and CBHI on Avicel, by measuring the amount of soluble sugars (e.g., as glucose equivalents) released from Avicel at an identical total enzyme concentration. Figure 3D shows that, at higher enzyme-to-cellulose ratio, CBHI has better hydrolytic efficiency than the polycatalytic CBHI complexes, but at the lower enzyme-to-cellulose ratios (Figure 3E, F), both CBHI/MNP−PAA and CBHI/MNP−PMAA exhibited significantly greater efficiency compared to the CBHI. Figure 3F shows that the soluble sugars released in 24 h increased by 500% in the case of CBHI/MNP−PMAA at 6% (w/v) of Avicel, when compared to the product produced at the same concentration of CBHI. We note here that the adsorption levels of CBHI complexes strongly depend on the concentration of enzymes and cellulose, due to their low binding capacity (Figure 3A−C and Figure S3, Supporting Information). In contrast, almost 100% of the CBHI adsorbed on the cellulose surface in the three different enzyme-to-cellulose ratios examined. The control experiments on the MNP−PAA and MNP−PMAA without enzymes show that the colloidal scaffolds alone do not have hydrolytic activity in degrading cellulose.

To compare the inherent hydrolytic activity between CBHI and CBHI−MNP complexes, we calculated the reaction productivity by normalizing the amount of released soluble sugar after 24 h, according to the actual fraction of enzyme complexes or enzymes bound on the cellulose. Figure 5 shows that, after correction, both the CBHI/MNP−PAA and CBHI/MNP−PMAA have significantly higher productivity than the CBHI at these enzyme concentrations, but the gap gradually decreases with increasing enzyme concentration. The extent of activity enhancement found with the complexes is remarkable, but somewhat puzzling. Individual CBHI molecules are known

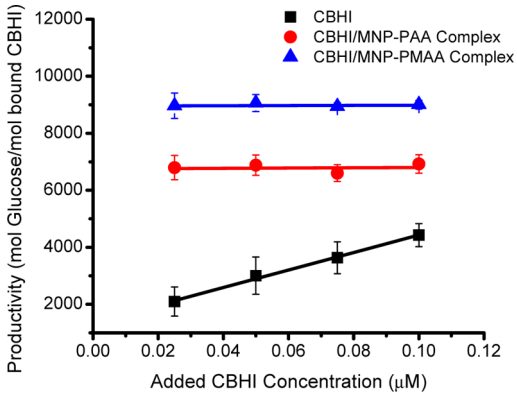

Figure 5. Effect of total enzyme concentration on the reaction productivities of CBHI complexes and CBHI. Amount of soluble sugar released was measured from the solutions after incubating CBHI or CBHI complexes with 20 mg/mL of Avicel for 24 h at 37 °C in 5 mM Tris-HCl buffer, pH 6.5. Productivity was determined by normalizing the amount of soluble sugars released with the amount of enzymes bound on the cellulose substrate.

to rely on processive motion on the track of the crystalline cellulose to carry out the hydrolytic reactions continuously and release the cellobiose.[40,41] Very unlikely, the large number of CBHI molecules on MNP−PAA or MNP−PMAA can coordinate their motions collectively to facilitate a similar, processive motion as a whole unit. Then, what are the possible mechanisms that facilitate the remarkable hydrolytic efficiency of CBHI complexes?

Careful examination of the adsorption and the hydrolysis kinetics (Figure 3) indicates that the hydrolytic reactions of the CBHI almost ceased within five hours at the low enzyme concentrations, suggesting that at these conditions most adsorbed CBHIs were trapped on the obstacles on the heterogeneous cellulose surface and lost their processive motions (i.e., processivity) at the late stage.[42] The so-called "jamming" of CBHI on crystalline cellulose is a known phenomenon, as found in a recent study using high-speed atomic force microscopy (HS-AFM).[43] The dissociation rate constants (k_{off}) for CBHI were previously reported with values in the range of 10^{-3} s^{-1}, corresponding to a half-life on Avicel around 10 min.[42] Therefore, regaining the processivity of jammed CBHI through the way of desorption and re-adsorption is relatively ineffective. Instead, accumulation of multiple CBHI molecules behind the blocked one leads to the elimination of the obstacle, and the coordinated action of the "on-site" clusters may be an effective mechanism to regain processivity of trapped CBHI: a cooperative behavior.[43] The probability of forming such clusters on the trapped sites depends on the concentration of mobile enzymes bound on the surface of cellulose. Therefore, adding more CBHI to the system will favor the temporal aggregation of multiple enzymes on the obstacle sites and facilitate the elimination of the obstacles for processive motion. This hypothesis seems to be supported by examining the hydrolytic reactions of Avicel by CBHI at higher concentrations (e.g., 0.5 μM), which shows the continuity of the reaction even after 24 h and the doubling of productivity of CBHI when the enzyme concentration increases from 0.1 to 0.5 μM (Figure S4, Supporting Information).

In contrast, the hydrolytic reactions of Avicel by polycatalytic CBHI complexes follow a different pattern from the CBHI (Figure 5). Even at very low enzyme concentrations, activities of

bound complexes remain high. Increasing the enzyme concentration contributes insignificantly to the productivity of the bound complexes (Figure 5), and Figure 3D−F shows that, in all experiments, the activity of the bound complexes did not prevail with time (slowed down substantially in less than ten hours). Apparently, the short-range processive motion of individual CBHI tethered to the flexible PMAA or PAA scaffolds is allowed, judging from the high productivity of the complexes. However, the complex may not have the processive motion or long-range mobility as a collective unit. For polycatalytic complexes, the effective concentration of CBHI in contact with cellulose largely depends on the grafting densities of enzymes in the complex rather than the bulk concentration of enzymes. The high local molarity of enzymes in our complexes seems to facilitate some cooperative behaviors similar to that found in the temporal clustering of the free enzymes in overcoming the obstacles. Consequently, at low total enzyme concentrations, especially, CBHI complexes have significant advantages relative to CBHI. The physical property of the supporting scaffolds also has the effect on the cooperative behaviors of the tethered enzymes. PMAA, which is more rigid than PAA, appears to be a better choice for the scaffold materials. However, the large polycatalytic complex lacks long-range surface mobility, and their extremely tight, polyvalent nature of the binding to the cellulose precludes desorption as an effective, alternative way to relocate the complexes on new substrate sites. Therefore, when the concentration of bound enzyme was increased to a level comparable to the local molarity of enzymes in the complexes, CBHI eventually becomes more effective (Figure S4, Supporting Information) by taking advantage of both the agility of individual processive motions and the cooperative mechanism in overcoming the obstacle sites to regain processivity.

Effect of Enzyme Grafting Densities and Particle Sizes on the Surface Adsorption and Hydrolytic Activities of the Polycatalytic CBHI complexes on Cellulose. On the basis of the proposed mechanism, the high local molarity of enzymes in the complexes plays an important role in enhancing the effectiveness of enzyme complexes at low total enzyme concentrations. We prepared two additional CBHI/MNP−PAA samples that have the same colloidal core but possess different grafting densities of CBHI on the surface (around 150 and 400 enzymes per complex) and compared their hydrolytic activities at the same total enzyme concentrations. Figure 6 shows how the hydrolytic activities of the CBHI complexes depended on the grafting densities of enzymes. Increasing the local concentration of enzymes in the complexes clearly enhances the activities of the polycatalytic complexes, but the maximum grafting density is limited by the conjugation method used and specific enzyme interactions. We also examined the CBHI complexes that have identical surface density of enzymes but have different core sizes. As expected, the complexes with smaller cores have larger binding capacity to Avicel (Figure S5, Supporting Information), presumably due to their smaller footprint. After correcting for their adsorption levels, the specific activities of different-sized complexes do not vary much (Figure S5, Supporting Information), indicating that the inherent reactivity of the polycatalytic complexes is mainly determined by the local organization of enzymes.

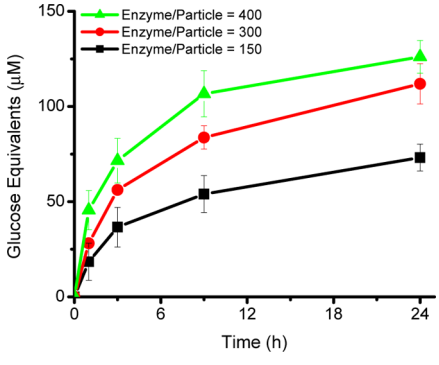

Figure 6. Effect of grafting density on the hydrolysis of the CBHI/MNP−PAA complex. The total enzyme concentration and Avicel concentration were kept constant at 0.025μM and 20 mg/mL, respectively, and incubation was at 37 °C in 5 mM Tris-HCl, pH 6.5. At the given times, the Avicel was separated from the enzyme complexes by sedimentation.

Trace the Motion of Individual CBHI Complexes on Cellulose Film Using Total Internal Reflection Fluorescence Microscopy (TIRFM). We used TIRFM to examine the adsorption/desorption and surface mobility of individual CBHI complexes on cellulose thin films, to confirm our findings derived from the experiments based on ensemble behavior. Avicel was first dissolved in ionic liquids, and the diluted solution was spun cast onto a microscope cover-slide and annealed under a controlled environment to prepare a smooth film of regenerated cellulose with a thickness of ∼50 nm and crystallinity of ∼80% (see Figure S6 (Supporting Information) for the atomic force microscopy (AFM) image of the film and Figure S7 (Supporting Information) for the wide-angle X-ray diffraction (WAXD) profile). CBHI/MNP−PMAA complexes were conjugated with fluorescein isothiocyanate (FITC) for fluorescence imaging and introduced into the buffer solution above the cellulose thin film. Under TIRFM, only the particles bound on the cellulose thin film (within ∼100 nm distance from the cover slide) are visible. Therefore, the adsorption and desorption of individual CBHI complexes on cellulose film can be readily followed using time-lapse TIRFM imaging, and their surface motions can be individually traced with great accuracy. Figure 7 shows a set of representative data on the adsorption of CBHI/MNP−PMAA onto regenerated cellulose thin film (see the Supporting Information for the movie that has been sped up 50 times). Once bounded, the complexes rarely desorbed from the cellulose surface in the time scale of the experiments (∼1 h), in agreement with the apparent dissociation constants measured. The time-dependent positions of individual complexes were analyzed, based on a particle-tracing program (CISMM Video Spot Tracker, http://www.cismm.org/downloads/), and corrected for the stage drifting (∼3 nm/s). Figure 8 shows the individual traces of 20 complexes after they bound on the cellulose film. Unlike the processive CBHI which moves as fast as 5 nm/s on the cellulose,[43] the CBHI complex as a whole unit is incapable of moving any large, detectable distance in our experiments. This supports our proposed mechanism in explaining the different hydrolytic reactivity found in the enzyme complexes.

CONCLUSIONS

The formation of polycatalytic clusters of cellulases on colloidal polymers increases the rate of hydrolytic reactions on cellulose but mainly at relatively low cellulase-to-cellulose ratios. At these conditions, the free enzymes are prone to get "jammed" at the obstacles on the cellulose surface. The polycatalytic complexes, on the other hand, facilitate effective polyvalent contacts between a high local molarity of enzymes and cellulose, for enhanced efficiency in the hydrolytic reactions. However, once bound, the

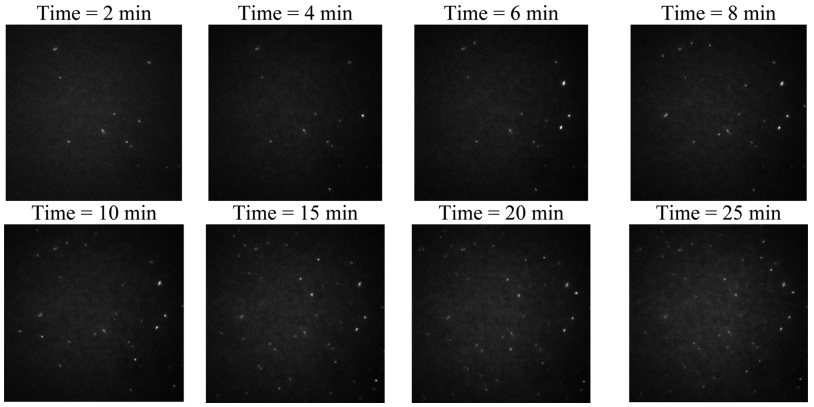

Figure 7. Time-dependent TIRF study on the adsorption and motion of CBHI/MNP−PMAA complexes on the cellulose thin film. The experiment was performed in 5 mM Tris HCl buffer at 37 °C. The images have a size of 87 μm × 87 μm.

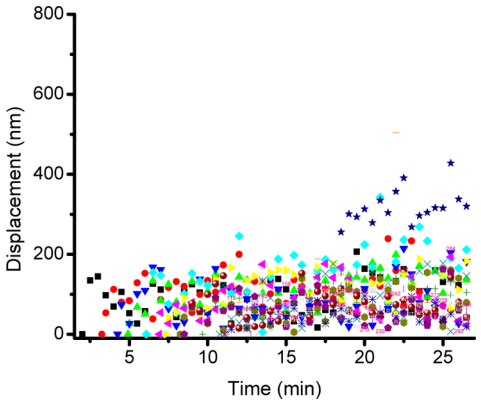

Figure 8. Displacement of individual CBHI/MNP−PMAA complexes from the original adsorption sites on the cellulose thin film.

polycatalytic complexes can only carry out reactions locally and not capable of relocating to new sites due to their lack of long-range surface mobility and their extremely tight binding. Therefore, at increased cellulase-to-cellulose ratios, free enzymes gradually become more effective due to their much higher binding capacity and presumably with the help of a cooperative mechanism that regains the processivity of trapped enzyme by the formation of clusters on-site to clear the barriers. The opportunity in the development of highly optimized polycatalytic complexes across different concentration ranges may come from the design of new nanoscaffolds that can indeed coordinate the motions of individual enzymes in the complex and that can couple the external forces to gain motility to speed up the overall enzymatic reactions.

EXPERIMENTAL SECTION

Materials. Cellulase mixture from *Trichoderma reesei* (Celluclast 1.5 L from Novozymes), β-glucosidase (Novozymes 188), glucose oxidase, horseradish peroxidase, papain, microcrystalline cellulose (Avicel, PH101), and 4-methylumbelliferyl β-D-cellobioside were purchased from Sigma-Aldrich. All other chemicals were of analytical grade and purchased from Fisher Scientific. CBHI was purified from cellulase mixture as described,[44] using GE FPLC equipped with ion exchange columns. The purity of CBHI and other individual enzymes was verified by their molecular weights using SDS-PAGE and by the very sensitive measurement of the specific activity against small chromogenic substrate 4-methylumbelliferyl β-D-cellobioside at 50 °C.[34] The extinction coefficient of 78800 M^{-1} cm^{-1} was used to determine the concentration of CBHI in solution.[44]

Synthesis of MNPs. In the synthesis of MNPs with a core size of ~200 nm, 1.350 g of $FeCl_3 \cdot 6H_2O$, 3.854 g of $NH_4 \cdot Ac$, and 0.4 g of sodium citrate were dissolved in 70 mL of ethylene glycol. The mixture was stirred vigorously for 1 h at 170 °C to form a homogeneous black solution, transferred into a Teflon-lined stainless-steel autoclave (100 mL capacity), and incubated at 200 °C for 16 h. The black product was washed with ethanol and separated from the solvent by using a magnet. The washing and separation steps were repeated several times. The final product was dispersed in ethanol for further use. In the synthesis of MNPs with a core size of ~100 nm, 1.08 g of $FeCl_3 \cdot 6H_2O$, 2.4 g of NaAc, and 0.25 g of sodium citrate were dissolved in 20 mL of ethylene glycol. The mixture was stirred vigorously for 0.5 h at room temperature to form a homogeneous dark red solution, transferred into a Teflon-lined stainless-steel autoclave (50 mL capacity), and incubated at 200 °C for 20 h. The washing and separation steps were the same as those in the synthesis of 200 nm MNPs.

Modification of MNPs with MPS. Modification of MNPs with MPS was achieved by adding 40 mL of ethanol, 10 mL of deionized water, 1.5 mL of $NH_3 \cdot H_2O$ and 0.3 g of MPS into the MNPs ethanol suspension and vigorously stirring the mixture for 24 h at 60 °C. The obtained product was separated by using a magnet and washed with ethanol to remove excess MPS. The resultant MNP-MPS nanoparticles were dried in a vacuum oven at 40 °C till constant weight.

Synthesis of MNP−PAA and MNP−PMAA Core/Shell Particles. Coating a PAA or PMAA layer onto MNP−MPS nanoparticles was performed by distillation−precipitation polymerization of AA or MAA in acetonitrile, with MBA as the cross-linker and AIBN as the initiator. Typically, 200 mg of MNP−MPS seed nanoparticles was dispersed in 160 mL of acetonitrile in a dried 250 mL single-necked flask and sonicated for 10 min. A mixture of 0.8 mL of AA or MAA, 89 mg of MBA, and 20 mg of AIBN was added to the flask to initiate the polymerization. The flask was submerged in a heating oil bath and attached with a fractionating column, Liebig condenser, and a receiver. The reaction mixture was heated from ambient temperature to the boiling state within 30 min, and the reaction was ended after about 80 mL of acetonitrile was distilled from the reaction mixture (in about 1 h). The MNP−PAA or MNP−PMAA was collected by magnetic separation and washed with ethanol to remove excess reactants and the polymer nanospheres (without a MNP core) from the side reactions.

Conjugation of Cellulase to MNP−PAA or MNP−PMAA Particles. CBHI was conjugated to MNP−PAA or MNP−PMAA using 1-ethyl-3-(3-dimenthylaminopropyl) carbodiimide hydrochloride (EDC) and *N*-hydroxysulfosuccinimide (Sulfo-NHS) coupling chemistry.[33] For conjugation, MNP−PAA or MNP−PMAA solutions were prepared in 0.50 M MES buffer at pH 6, with a concentration around 10^{11} particles/mL. Amounts of 2 mg of EDC and 2 mg of Sulfo-NHS were then added into 1 mL of particle suspension, and the solution was incubated at room temperature with mixing for 10 min. The activated particles were separated from the solution by a magnetic rack, washed, and added into 2 mg/mL of CBHI solution in 12 mM PBS buffer at pH 7.4. The mixture was incubated at room temperature in a rotator for 6 h

followed by washing with 5 mM Tris-HCl buffer five times to remove unbound proteins. The concentration of CBHI bound to the particles was calculated by comparing the specific activity against 4-methylumbelliferyl β-D-cellobioside in 50 mM sodium acetate at 50 °C with that of the CBHI solutions with the known concentration.

Adsorption and Activity Experiments for CBHI. An amount of 1 mL of CBHI solution in 5 mM Tris-HCl at pH 6.5 was mixed with 20−60 mg of Avicel in a centrifuge tube and incubated at 37 °C temperature on a mixer. At the given incubation time, the Avicel was pelleted by centrifugation at 14 000 rpm for 3 min, and the supernatant was withdrawn. The concentration of unbound CBHI in the supernatants was determined by measuring A_{280} and the specific activity against 4-methylumbelliferyl β-D-cellobioside. An aliquot was taken for reducing sugar analysis based on the glucose oxidase (GOX)/horseradish peroxidase (HRP) method and using HPLC.[21,45] All experiments were done in triplicate.

Adsorption and Activity Experiments for CBHI/MNP−PAA or CBHI/MNP−PMAA Complexes. An amount of 1 mL of CBHI/MNP−PAA or CBHI/MNP−PMAA solution in 5 mM Tris-HCl at pH 6.5 was mixed with 20−60 mg of Avicel in a centrifuge tube and incubated at 37 °C temperature on a mixer. At the given incubation time, a tube was removed from the mixer and put on a rack for 5 min to let the Avicel sediment. Due to their small sizes, the unbound CBHI/MNP−PAA or CBHI/MNP−PMAA remained fully suspended in solution (up to hours) and was pipetted out to separate unbound enzyme complexes from the Avicel. After washing once, the concentration of absorbed CBHI complexes on Avicel was then determined by comparing the specific activity against 4-methylumbelliferyl β-D-cellobioside with that of stock solution with a predetermined amount of CBHI. The suspension of unbounded enzyme complexes was then pelleted by centrifugation at 14 000 rpm for 3 min, and the supernatant was withdrawn to determine the concentration of reducing sugars. Adsorption isotherms were determined with 20 mg/mL of Avicel.

Surface Mobility of CBHI Complexes on Cellulose Thin Film Studied by TIRF Microscopy. Cellulose films (∼50 nm) were prepared by spin coating of 5 wt % cellulose solution in 1-ethyl 3-methyimidazolium acetate on a pre-cleaned coverslip.[46−48] The coverslip was placed on a glass slide with the cellulose film facing inward and affixed by double-sided tapes to leave a small gap between the film and the surface of the glass slide. A dilute solution of FITC tagged CBHI/MNP−PMAA complexes (∼50 μL) was then introduced into the gap and in contact with the cellulose film. The interface between the complex solution and the cellulose thin film was focused and imaged using a Nikon TIRF microscope equipped with an oil immersion TIRF lens (1.49 NA, 100×, Nikon) and an Andor 897 iXon EMCCD camera. Sample environment was maintained at a temperature of 37 ± 3 °C using an environmental chamber, and TIRF images were taken at an interval of 5−30 s. Image analysis was performed by using NIH ImageJ software, and the surface mobility of complexes was analyzed by using CISMM Video Spot Tracker program.

■ ASSOCIATED CONTENT

Supporting Information

FPLC chromatography, SDS-PAGE gel, and activity assays of cellulases. Adsorption behaviors of CBHI and CBHI complexes, hydrolytic activity of CBHI at different enzyme concentrations, and effect of sizes of the complexes on the adsorption and hydrolysis kinetics. AFM image and WAXS pattern of cellulose thin films. This material is available free of charge via the Internet at http://pubs.acs.org.

■ AUTHOR INFORMATION

Corresponding Author

*E-mail: ylin@ims.uconn.edu.

Notes

The authors declare no competing financial interest.

■ ACKNOWLEDGMENTS

This work was supported by the US Department of Energy, Office of Basic Energy Sciences, Division of Materials Sciences and Engineering (DE-SC0005039). Y.L. acknowledges a senior visiting scholarship provided by Fudan University and the University of Connecticut Confocal Microscopy Facility and Carol Norris for training, advice, and use of instrumentation. C.W. acknowledges the support from the National Science and Technology Key Project of China (Grant No. 2012AA0202204).

■ REFERENCES

(1) Hill, J.; Nelson, E.; Tilman, D.; Polasky, S.; Tiffany, D. *Proc. Natl. Acad. Sci. U.S.A.* **2006**, *103*, 11206−11210.
(2) Himmel, M. E.; Ding, S.-Y.; Johnson, D. K.; Adney, W. S.; Nimlos, M. R.; Brady, J. W.; Foust, T. D. *Science (Washington, DC, U.S.)* **2007**, *315*, 804−807.
(3) Ding, S.-Y.; Liu, Y.-S.; Zeng, Y.; Himmel, M. E.; Baker, J. O.; Bayer, E. A. *Science (Washington, DC, U.S.)* **2012**, *338*, 1055−1060.
(4) Chang, M. C. Y. *Curr. Opin. Chem. Biol.* **2007**, *11*, 677−684.
(5) Doi, R. H.; Kosugi, A. *Nat. Rev. Microbiol.* **2004**, *2*, 541−551.
(6) Staahlberg, J.; Johansson, G.; Pettersson, G. *Bio/Technology* **1991**, *9*, 286−90.
(7) Nidetzky, B.; Claeyssens, M.; Steiner, W. *Biotechnol. Pulp Pap. Ind., Proc.* **1996**, 537−542.
(8) Jalak, J.; Kurasin, M.; Teugjas, H.; Vaeljamaee, P. *J. Biol. Chem.* **2012**, *287*, 28802−28815.
(9) Bayer, E. A.; Lamed, R. *J. Bacteriol.* **1986**, *167*, 828−36.
(10) Fierobe, H.-P.; Bayer, E. A.; Tardif, C.; Czjzek, M.; Mechaly, A.; Belaich, A.; Lamed, R.; Shoham, Y.; Belaich, J.-P. *J. Biol. Chem.* **2002**, *277*, 49621−49630.
(11) Ding, S. Y.; Xu, Q.; Crowley, M.; Zeng, Y.; Nimlos, M.; Lamed, R.; Bayer, E. A.; Himmel, M. E. *Curr. Opin. Biotechnol.* **2008**, *19*, 218−227.
(12) Bayer, E. A.; Belaich, J. P.; Shoham, Y.; Lamed, R. *Annu. Rev. Microbiol.* **2004**, *58*, 521−554.
(13) Fierobe, H.-P.; Mingardon, F.; Mechaly, A.; Belaich, A.; Rincon, M. T.; Pages, S.; Lamed, R.; Tardif, C.; Belaich, J.-P.; Bayer, E. A. *J. Biol. Chem.* **2005**, *280*, 16325−16334.
(14) Hammel, M.; Fierobe, H.-P.; Czjzek, M.; Kurkal, V.; Smith, J. C.; Bayer, E. A.; Finet, S.; Receveur-Brechot, V. *J. Biol. Chem.* **2005**, *280*, 38562−38568.
(15) Tebeka, I. R. M.; Silva, A. G. L.; Petri, D. F. S. *Langmuir* **2009**, *25*, 1582−1587.
(16) Ho, K. M.; Mao, X.; Gu, L.; Li, P. *Langmuir* **2008**, *24*, 11036−11042.
(17) Kim, D.-M.; Umetsu, M.; Takai, K.; Matsuyama, T.; Ishida, N.; Takahashi, H.; Asano, R.; Kumagai, I. *Small* **2011**, *7*, 656−664.
(18) Hirsh, S. L.; Bilek, M. M. M.; Nosworthy, N. J.; Kondyurin, A.; dos Remedios, C. G.; McKenzie, D. R. *Langmuir* **2010**, *26*, 14380−14388.
(19) Cho, E. J.; Jung, S.; Kim, H. J.; Lee, Y. G.; Nam, K. C.; Lee, H.-J.; Bae, H.-J. *Chem. Commun. (Cambridge, U. K.)* **2012**, *48*, 886−888.
(20) Blanchette, C.; Lacayo, C. I.; Fischer, N. O.; Hwang, M.; Thelen, M. P. *PLoS One* **2012**, *7*, e42116.
(21) MacKenzie, K. J.; Francis, M. B. *J. Am. Chem. Soc.* **2013**, *135*, 293−300.
(22) Liao, H.; Chen, D.; Yuan, L.; Zheng, M.; Zhu, Y.; Liu, X. *Carbohydr. Polym.* **2010**, *82*, 600−604.
(23) Nidetzky, B.; Steiner, W.; Claeyssens, M. *Biochem. J.* **1994**, *303* (Pt 3), 817−23.
(24) Boraston, A. B.; Bolam, D. N.; Gilbert, H. J.; Davies, G. J. *Biochem. J.* **2004**, *382*, 769−781.
(25) Poon, D. K. Y.; Withers, S. G.; McIntosh, L. P. *J. Biol. Chem.* **2007**, *282*, 2091−2100.
(26) Nidetzky, B.; Steiner, W.; Hayn, M.; Claeyssens, M. *Biochem. J.* **1994**, *298*, 705−710.
(27) Beckham, G. T.; Bomble, Y. J.; Matthews, J. F.; Taylor, C. B.; Resch, M. G.; Yarbrough, J. M.; Decker, S. R.; Bu, L. T.; Zhao, X. C.;

McCabe, C.; Wohlert, J.; Bergenstrahle, M.; Brady, J. W.; Adney, W. S.; Himmel, M. E.; Crowley, M. F. *Biophys. J.* **2010**, *99*, 3773−3781.
(28) Divne, C.; Stahlberg, J.; Teeri, T. T.; Jones, T. A. *J. Mol. Biol.* **1998**, *275*, 309−325.
(29) Ting, C. L.; Makarov, D. E.; Wang, Z. G. *J. Phys. Chem. B* **2009**, *113*, 4970−4977.
(30) Igarashi, K.; Koivula, A.; Wada, M.; Kimura, S.; Penttila, M.; Samejima, M. *J. Biol. Chem.* **2009**, *284*, 36186−36190.
(31) Ma, W.; Xu, S.; Li, J.; Guo, J.; Lin, Y.; Wang, C. *J. Polym. Sci., Part A: Polym. Chem.* **2011**, *49*, 2725−2733.
(32) Zhang, Y.; Yang, Y.; Ma, W.; Guo, J.; Lin, Y.; Wang, C. *ACS Appl. Mater. Interfaces* **2013**, *5*, 2626−2633.
(33) Staros, J. V.; Wright, R. W.; Swingle, D. M. *Anal. Biochem.* **1986**, *156*, 220−2.
(34) Heptinstall, J.; Stewart, J. C.; Seras, M. *Enzyme Microb. Technol.* **1986**, *8*, 70−4.
(35) Liu, Y.-S.; Baker, J. O.; Zeng, Y.; Himmel, M. E.; Haas, T.; Ding, S.-Y. *J. Biol. Chem.* **2011**, *286*, 11195−11201.
(36) Chanzy, H.; Henrissat, B.; Vuong, R.; Schulein, M. *FEBS Lett.* **1983**, *153*, 113−118.
(37) Hall, M.; Bansal, P.; Lee, J. H.; Realff, M. J.; Bommarius, A. S. *Febs J.* **2010**, *277*, 1571−1582.
(38) Umpleby, R. J., II; Baxter, S. C.; Chen, Y.; Shah, R. N.; Shimizu, K. D. *Anal. Chem.* **2001**, *73*, 4584−4591.
(39) Sugimoto, N.; Igarashi, K.; Wada, M.; Samejima, M. *Langmuir* **2012**, *28*, 14323−14329.
(40) Fox, J. M.; Levine, S. E.; Clark, D. S.; Blanch, H. W. *Biochemistry* **2012**, *51*, 442−452.
(41) Bu, L. T.; Nimlos, M. R.; Shirts, M. R.; Stahlberg, J.; Himmel, M. E.; Crowley, M. F.; Beckham, G. T. *J. Biol. Chem.* **2012**, *287*, 24807−24813.
(42) Kurasin, M.; Vaeljamaee, P. *J. Biol. Chem.* **2011**, *286*, 169−177.
(43) Igarashi, K.; Uchihashi, T.; Koivula, A.; Wada, M.; Kimura, S.; Okamoto, T.; Penttilae, M.; Ando, T.; Samejima, M. *Science (Washington, DC, U. S.)* **2011**, *333*, 1279−1282.
(44) Medve, J.; Lee, D.; Tjerneld, F. *J. Chromatogr., A* **1998**, *808*, 153−165.
(45) Huggett, A. S.; Nixon, D. A. *Lancet* **1957**, *273*, 368−70.
(46) Swatloski, R. P.; Spear, S. K.; Holbrey, J. D.; Rogers, R. D. *J. Am. Chem. Soc.* **2002**, *124*, 4974−4975.
(47) Cao, Y.; Li, H.; Zhang, Y.; Zhang, J.; He, J. *J. Appl. Polym. Sci.* **2010**, *116*, 547−554.
(48) Josefsson, P.; Henriksson, G.; Wagberg, L. *Biomacromolecules* **2008**, *9*, 249−254.